GEOPHYSICAL RESEARCH LETTERS, VOL. 26, NO. 23, PAGES 3569-3572, DECEMBER 1, 1999

Subionospheric VLF Signatures of Oblique (Nonducted) Whistler-Induced Precipitation

M. P. Johnson, U. S. Inan, and D. S. Lauben

STAR Laboratory, Stanford University, Stanford, CA 94305

Abstract. Subionospheric very low frequency (VLF) signal perturbations observed at multiple sites in association with individual lightning discharges exhibit onset delays which steadily increase with increasing L-value. The timing of the onsets and the inferred spatial extent (~1000 km) of the ionospheric disturbance are consistent with those expected for electron precipitation induced by obliquely propagating (i.e., nonducted) whistlers.

Introduction

Lightning-induced electron precipitation (LEP) is a well established means of loss of the trapped radiation belt electrons caused by resonant whistler wave-particle interactions. There is now extensive experimental evidence for direct precipitation of individual bursts of energetic electrons in association with individual lightning discharges as measured on satellites, rockets, and by means of VLF remote sensing of associated ionospheric disturbances [*Voss et al.*, 1998 and associated references therein]. Previous theoretical [e.g., *Inan et al.*, 1989] and experimental [e.g., *Burgess and Inan*, 1993] work on the LEP phenomena has mostly emphasized interactions with 'ducted' whistler waves which propagate in field-aligned ducts of enhanced ionization. While the possibility of resonant pitch angle scattering by obliquely propagating 'nonducted' whistlers has been recognized [*Jasna et al.*, 1992], the first comprehensive quantitative model of the transient precipitation of bursts of energetic electrons by oblique whistlers launched by individual lightning flashes has only recently been realized [*Lauben et al.*, 1999].

Ground-based VLF remote sensing yields information about the nighttime ionospheric D region conductivity altered by the enhanced secondary ionization produced by ~50 to 500 keV precipitating energetic electrons. VLF transmitter signals propagate between the surface of the earth and the D region (Figure 1b), and changes in the conductivity profile along the great circle path (GCP) of propagation (Figure 1c) perturb the received amplitude and/or phase. These perturbations, known as LEP VLF events (Figures 1d and 1e), are characterized by (i) a characteristic onset delay Δt (a few hundred ms up to 1s) with respect to the causative sferic (Figure 1f) due to the magnetospheric travel time of the outgoing whistler wave and the pitch angle scattered particles (Figure 1a): (ii) an onset duration, t_d (typically .5–1.5 s) representing the duration of the precipitation burst, during which the VLF event magnitude increases due to continuing generation of secondary ionization: and (iii) a recovery period of 10-100 s following the termination of the precipitation burst, as the ionization returns from enhanced levels back to pre-event levels.

For LEP VLF events induced by ducted whistlers, Δt and t_d depend on the magnetic latitude of propagation (i.e., L-shell) and the ambient magnetospheric cold plasma density [*Inan and Carpenter*, 1986], but the required presence of a magnetospheric duct nevertheless quantizes the values of these parameters for any given case. In contrast, scattering by obliquely propagating whistlers (which permeate a wide range of field lines) leads to precipitation over an extended region, with a continuum of onset delays and durations as a function of latitude [*Lauben et al.*, 1999].

We report direct experimental confirmation of several predictions of *Lauben et al.* [1999]: (i) bursts of electrons precipitated at different field lines arrive at the ionosphere with delays (with respect to the causative lightning flash) steadily increasing with increasing L-value, (ii) ionospheric regions disturbed in individual events may have spatial extents of up to ~1000 km and are poleward-displaced in latitude with respect to the causative flash, and (iii) the peak precipitation fluxes induced by oblique whistlers are at least as intense as those produced by ducted waves. Our results constitute the first direct experimental evidence of LEP events produced by nonducted waves. Since most of the wave energy launched

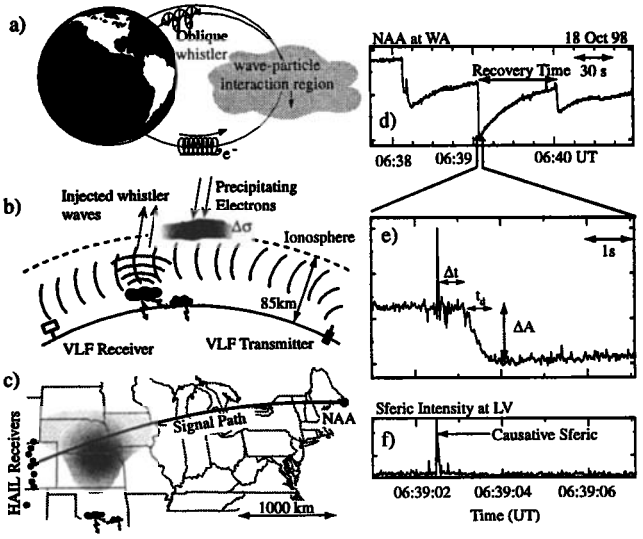

Figure 1. (a) An oblique whistler wave is launched into the magnetosphere. (b) Wave-particle interaction near the equatorial plane scatters trapped electrons which then precipitate and cause secondary ionization. (c) The D region ionospheric disturbance perturbs VLF signals propagating underneath. (d-f) An example LEP event with characteristic onset delay (with respect to the causative sferic) and duration.

Paper number 1999GL010706.
0094-8276/99/1999GL010706$05.00

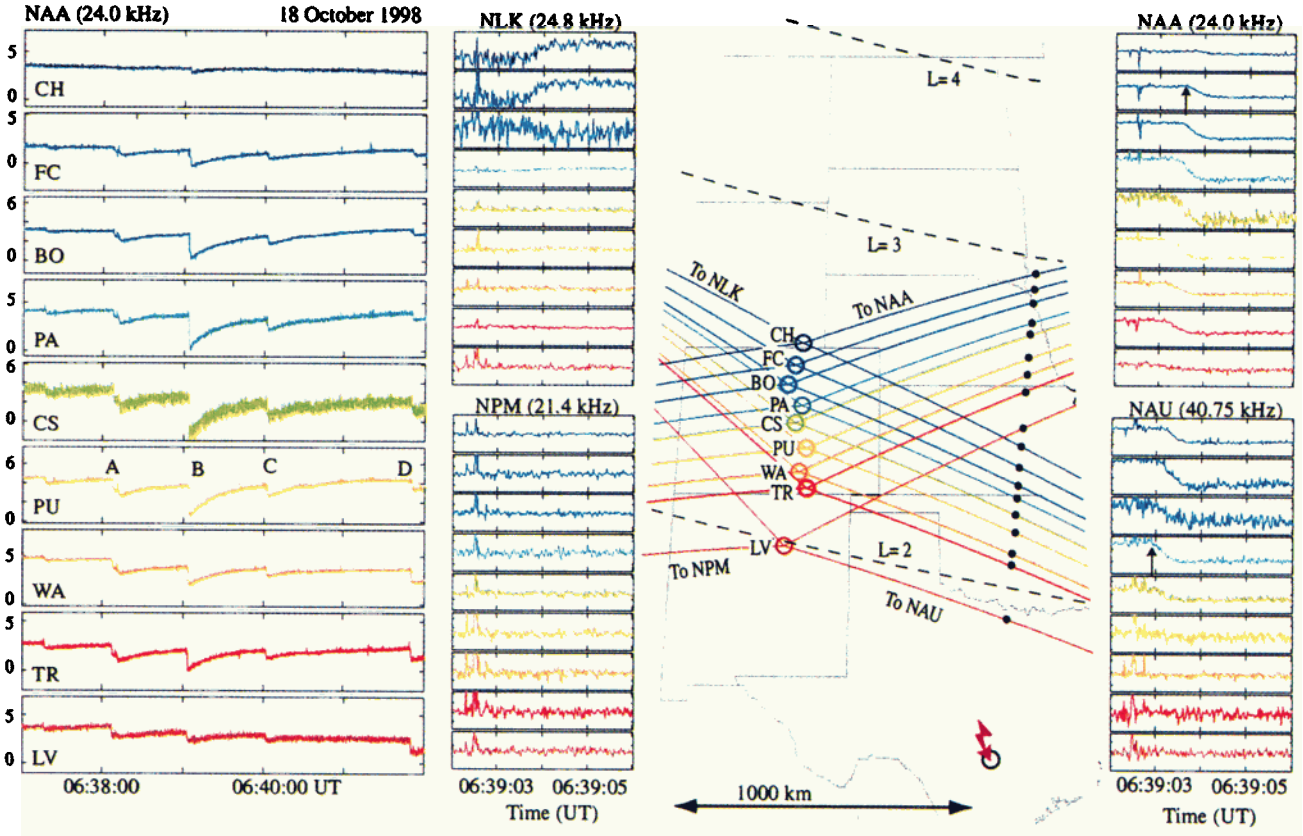

Figure 2. A five minute record of the received amplitude (in ~7 dB windows) from NAA at the nine HAIL sites is shown on the left, with four VLF events labeled A–D. The map shows the locations of the HAIL sites, together with color-coded GCPs from the four VLF transmitters monitored. Footprints of the L=2, 3 and 4 field lines are shown for reference. Event B amplitude is plotted (in 4 dB windows) with an expanded time scale for each of the transmitter signals. The causative lightning at ~6:39:02.5 UT was near Austin Texas. Intersection points of the GCPs and the magnetic longitude of the causative discharge are shown as black dots.

into the magnetosphere propagates in the nonducted mode, our observations suggest that the LEP process may be a significant contributor to the loss of radiation belt particles on a global scale.

Description of the Experiment

The VLF data were collected during the summer of 1998 by a set of nine VLF receivers with ~65 km spacing (Figure 2a) constituting the Holographic Array for Ionospheric Lightning research (HAIL) system. The HAIL array provides sufficient spatial resolution [*Chen et al.*, 1996] for the measurement of lightning-associated ionospheric disturbances and also allows coverage of a large part of the Midwestern thunderstorm centers by continuously observing VLF transmitter signals from Washington, Maine, Hawaii, and Puerto Rico. A mesh grid of GCPs on each side of the array is used to assess the spatial properties of these disturbances.

At each receiver the wideband signal detected by a 1.7 x 1.7m^2 magnetic loop antenna is bandpass filtered to a range of 9 - 45 kHz and sampled at 100 kHz with triggers provided by GPS timing. This broadband signal is subsequently rectified, averaged, and recorded with 20 ms resolution to allow the unambiguous detection of occurrence times and durations of sferics radiated by lightning discharges. The receivers digitally down-convert the individual VLF transmitter signals and record the demodulated amplitude and phase with 20 ms and 100 ms resolution, respectively, typically during 01:00 to 13:00 UT when most of the observed VLF paths are in the nighttime sector. GPS receivers provide absolute timing accuracy to a greater degree than the sample rate, thereby providing a stable reference for the phase demodulation. Sferic noise from local thunderstorms necessitates longer averaging period for phase data, making the amplitude data more suitable for detailed timing comparisons. The phase data (not shown) for the cases studied here are generally consistent with the conclusions extracted from amplitude data.

Data from the National Lightning Detection Network (NLDN) provides the time, location, and peak current of most CG lightning discharges [*Orville*, 1994], and is used in this work to locate the discharges associated with the LEP events.

Case Study: October 18, 1998

On eleven days in October 1998, HAIL data from multiple receivers clearly show LEP VLF event activity on the NAA transmitter signal. Of these eleven, repeated (>10 in one hour) and clearly identifiable (>0.5 dB) LEP VLF events occur on six days. In particular, several tens of events observed with the HAIL array on October 18 were large (several dB), and were individually imaged with the array

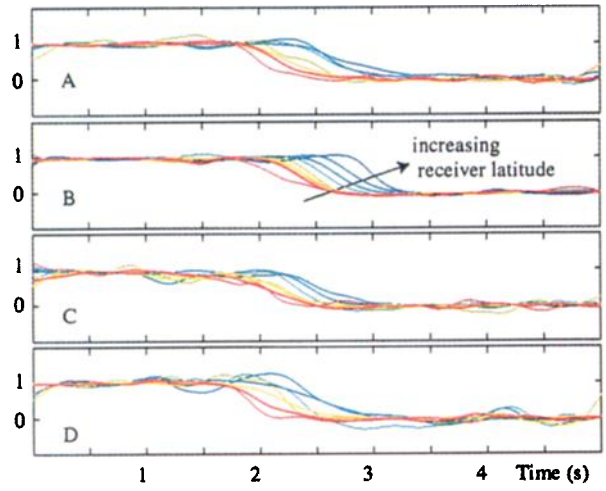

Figure 3. Normalized and filtered high resolution (20 ms) data (linear scale) for the nine NAA–HAIL signals superimposed for the events A–D from Figure 2, illustrating the increase in onset delay with increasing path latitude.

on three sets of VLF paths, suggesting a massive ionospheric disturbance region. The left-hand panel of Figure 2 shows a five minute sequence of VLF amplitude events, marked A–D, from several disturbances on the NAA signal. Although the event magnitudes vary along the array for each event, relative values of the amplitude changes at different sites along the array were similar for the series of different events, indicating that the causative ionospheric disturbances were similar in location and size.

Event 'B' from Figure 2 (at ~6:39:03 UT), when expanded for the WA receiver, shows the characteristic recovery to the ambient level (Figure 1d) and the characteristic onset delay and duration with respect to the causative sferic (Figures 1e and 1f). Data from NLDN identified only two discharges in the U.S. during the second containing the causative sferic, both located near Austin Texas, occurring at 6:39:02.487 and 6:39:02.532 UT, with peak currents of ~15kA. Other events in the sequence are also associated exclusively with observed discharges in central Texas.

High-resolution amplitude data from all four VLF transmitters recorded at the nine HAIL receivers are plotted in Figure 2 for a four second period around the event B onset. While ionospheric disturbances with ~100 km spatial extents (e.g., those involved in early/fast VLF events) are typically observed at two or three of the HAIL receivers [*Johnson et al.*, 1999], in this case all of the NAA–HAIL paths and the upper five NAU–HAIL were perturbed, indicating a disturbance of much larger extent located to the east of the array. The absence of events on the lower four NAU–HAIL paths (despite being closer to the causative discharge), indicates a poleward-displaced precipitation zone, as predicted by *Lauben et al.* [1999]. While the NPM–HAIL paths are not perturbed, the northernmost two NLK–HAIL paths were affected, suggesting that the disturbance had a wider extent in longitude at higher latitudes.

A striking feature of the data is the steadily increasing onset delay with increasing geomagnetic latitude of the affected paths. The lowest path to be significantly affected, NAU–PA, has an onset time for event B marked with an arrow in Figure 3. In comparison, the corresponding onset occurs over ~0.5 s later on the NAA–FC path. To better illustrate the different onset times, filtered and normalized amplitude signatures from NAA for events A–D are superimposed in Figure 3. In each of the cases, the onset delay increased with receiver latitude. For the best defined case, event B, we have a remarkably well defined set of curves with onset delay increasing monotonically with latitude. This case is analyzed quantitatively in the following section.

Comparison with Model Results

The distinctly different onset delays indicate that the various VLF paths respond to ionospheric disturbance regions that are activated at different times. Thus, the VLF amplitude changes seen on the different paths *cannot* be due to subionospheric VLF scattering from a single localized ionospheric disturbance, as produced (for example) near the footprint of a whistler-mode duct. Instead, the continuum of onset delays steadily increasing with geomagnetic latitude agrees remarkably well with the predictions of *Lauben et al.* [1999] who used a quantitative model of oblique-whistler-induced electron precipitation to determine the location and shape of ionospheric disturbances caused by individual lightning discharges occurring at mid-latitudes. Typical plasmaspheric conditions were considered for lightning discharges with peak currents of ~10 kA, and precipitated fluxes of electrons with energies greater than 100 keV (sufficient to cause secondary ionization at altitudes below 100 km) were calculated for source lightning discharges at different latitudes. The resulting precipitation region for a source lightning discharge at the location of the causative discharge for event B is shown in Figure 4a. For a simple tilted

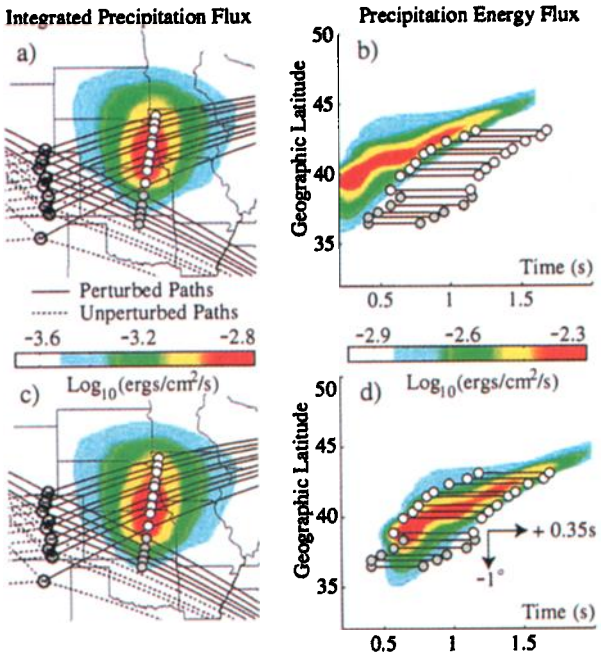

Figure 4. (a) *Lauben et al.* [1999] model predictions of time-integrated precipitation flux for E> 100 keV due to a 10 kA peak current discharge at the location of the causative discharge for event 'B'. (b) Corresponding flux plotted vs. geographic latitude and time, LEP event onset times and durations for event 'B' superimposed. (c) and (d): Same as above, but shifted southward by 1° and increased in time by 0.35 s.

dipole model and neglecting any longitudinal gradients in the earth's magnetic field or cold plasma density, the precipitation region is symmetric in geomagnetic longitude. The energy-flux deposition as a function of time and latitude is shown in Figure 4b and describes the manner in which the different paths of the precipitation region appear in time. In the *Lauben et al.* [1999] model, temporal evolution of the precipitation and the location in latitude of the region (for a given source location) is a function of assumed cold plasma gradients and densities. While we do not have in hand an independent measure of these parameters, we can compare the measured and predicted onset delays in order to estimate the latitudinal location of the precipitation region for this case. The onset delays and durations measured for event B on the different HAIL paths are shown in circles in Figure 4b, with the geomagnetic latitude for each path determined as the point of intersections of the constant longitude line with the GCP of interest.

The measured onset delays and durations in Figure 4b have the same general latitudinal variation as those predicted, although the predicted flux appears earlier in time and higher in latitude. The higher-than-predicted onset delays indicate that the magnetospheric cold plasma density values were higher than those used in *Lauben et al.* [1999], resulting in longer travel times for both the waves (whistler-mode refractive index is proportional to the square root of electron density) and particles (gyroresonant electron energies are lower for higher values of refractive index). The fact that the predicted precipitation region is located at higher latitudes implies that the actual oblique whistler-mode raypaths were confined to somewhat lower L-shells, and thus that the radial (i.e., L-shell) variation of the magnetospheric cold plasma density was more rapid than that used in *Lauben et al.* [1999]. The raypath configuration is determined primarily by the gradients of the static magnetic field, which does not exhibit significant day-to-day variations within the plasmasphere, and cold plasma density, which varies day-to-day depending on the geomagnetic activity, plasmapause location and local time [*Carpenter and Anderson*, 1992].

A simple shift of 1° in latitude and 0.35 s in time brings the measured onset durations (indicated by two circles marking the beginning and end of onset with a line drawn between them) in good agreement with those predicted, as shown in Figure 4d. Implementing this same 1° shift in latitude places the precipitation region solidly on the NAA–HAIL paths, as shown in Figure 4c. The association of the calculated ionospheric disturbance shape with the distribution of perturbed paths is quite remarkable, for example accounting for the fact that the middle NAA-HAIL paths have the largest signal perturbations, and that the lower four NAU paths are not perturbed.

On the other hand, the placement of the disturbance as shown in Figure 4c suggests that none of the NLK paths (arriving at HAIL from the east) should be perturbed, although the NLK-CH and NLK-FC signals clearly exhibited this event. In this context, it is important to note that the disturbance region shown in Figure 4c is calculated by neglecting any azimuthal ionospheric and magnetospheric plasma gradients and by assuming the energetic particle distribution to be uniform in latitude. Realistic variations in both of these parameters can both displace and distort the precipitation region.

Summary

Subionospheric VLF signatures of individual lightning-induced precipitation events observed at multiple distributed sites exhibit increasing onset delays with increasing geomagnetic latitude, in a manner similar to that expected on the basis of a quantitative model, thus providing the first clear evidence of precipitation of radiation belt electrons by non-ducted, obliquely propagating whistler waves launched by lightning. Comparison of measurements and theory confirm that extensive magnetospheric regions can be affected by individual lightning discharges, producing enhanced secondary ionization in regions ~1000 km in lateral extent, displaced in latitude with respect to the source lightning, and exhibiting a shape with a broader azimuthal extent at higher latitudes. Our results suggest that the lightning-induced electron precipitation (LEP) process is likely to be an important contributor to the loss of radiation belt electrons on a global scale, since oblique whistler waves are naturally excited under all magnetospheric conditions, and fill large regions of the magnetosphere without the need for the presence of field-aligned 'ducts' of enhanced ionization. On the other hand, the particular properties of a lightning flash that lead to LEP production is yet to be determined.

Acknowledgments. This work was supported under the National Science Foundation and the Office of Naval Research under grants ATM-9528173 and N00014-94-1-0100. The authors are indebted to the many high school teachers and students involved in the support of the HAIL array. We thank K. Cummins of Global Atmospherics, Inc. for allowing us to use the NLDN data.

References

Burgess W. C., and U. S. Inan, The role of ducted whistlers in the precipitation loss and equilibrium flux of radiation belt electrons, *J. Geophys. Res.*, 98, 15643-65, 1993.

Carpenter, D. L. and R. R. Anderson, An ISEE/whistler model of equatorial electron density in the magnetosphere, *J. Geophys. Res.*, 97, 1097-108, 1992.

Chen, J., U. S. Inan, and T. F. Bell, VLF strip holographic imaging of lightning-associated ionospheric disturbances, *Radio Science*, 31, 335-48, 1996.

Inan, U. S., and D. L. Carpenter, On the correlation of whistlers and associated subionospheric VLF/LF perturbations, *J. Geophys. Res.*, 91, 3106-16, 1986.

Inan, U. S., M. Walt, H. D. Voss, and W. L. Imhof, Energy spectra and pitch angle distributions of lightning-induced electron precipitation: analysis of an event observed on the S81-1 (SEEP) Satellite, *J. Geophys. Res.*, 94, 1379, 1989.

Jasna, D., U. S. Inan,and T. F. Bell, Precipitation of suprethermal (100 eV) electrons by oblique whistler waves, *Geophys. Res. Lett.*, 19, 1639-42, 1992.

Johnson, M. P., U. S. Inan, and S. J. Lev-Tov, Scattering pattern of lightning-induced ionospheric disturbances associated with early/fast VLF events, *Geophys. Res. Lett.*, 26, 2363-66, 1999.

Lauben, D. S., U. S. Inan, and T. F. Bell, Poleward-displaced electron precipitation from lightning-generated oblique whistlers, *Geophys. Res. Lett.*, 26, 2633-36, 1999.

Orville, R.E., Cloud-to-Ground Lightning discharge characteristics in the contiguous United States: 1989-1991, *J. Geophys. Res.*, 99, 10833-41, 1994.

Voss, H. D., M. Walt, W. L. Imhof, J. Mobilia, and U. S. Inan, Satellite observations of lightning-induced electron precipitation, *J. Geophys. Res.*, 103, 11725-44, 1998.

M. P. Johnson, STARLab, 306 Packard Bldg., Stanford, CA 94305.

(Received June 29, 1999; revised August 30, 1999; accepted September 7, 1999.)